Specific Heat Capacity at Constant Volume for $\{x NH_3 + (1 - x)H_2O\}$ at Temperatures from 300 to 520 K and Pressures to 20 MPa

Joseph W. Magee* and Noboru Kagawa†

Physical and Chemical Properties Division, Chemical Science and Technology Laboratory, National Institute of Standards and Technology, 325 Broadway, Boulder, Colorado 80303

Specific heat capacities at constant volume (c_V) of $\{x NH_3 + (1 - x)H_2O\}$ ($x \approx 0.7, 0.8, 0.9$) mixtures were measured with an adiabatic calorimeter. Temperatures ranged from 300 K to 520 K, and pressures ranged from 3 MPa to 20 MPa. Measurements were conducted on single-phase liquid and compressed gaseous samples. The mixtures were gravimetrically prepared from high-purity substances and verified by chemical analysis. Density was reported for initial and final end points during each calorimetric experiment. The principal sources of uncertainty are the temperature rise measurement and the change-of-volume work adjustment. The expanded relative uncertainty (with a coverage factor $k = 2$ and thus a 2-standard-deviation estimate) for c_V is estimated to be 1% for liquid phase and 4% for gaseous results, and for density it is 0.2%.

Introduction

Thermodynamic properties of a fluid may be calculated from a knowledge of its ideal-gas properties and an accurate equation of state. Heat capacities derived in this manner, however, often lack sufficient accuracy since the calculation involves integration of the isochoric curvature $(\partial^2 p/\partial T^2)_\rho$ as in the equation

$$c_V - c_V^\circ = -T \int_0^\rho \left(\frac{\partial^2 P}{\partial T^2}\right)_\rho \frac{d\rho}{\rho^2} \qquad (1)$$

where c_V° is the ideal-gas heat capacity. The quantity $(\partial^2 p/\partial T^2)_\rho$ is known to possess small absolute values except in the vicinity of the critical point and is very difficult to measure accurately. For compressed liquid states, additional data are required to apply eq 1, including the vapor pressure and enthalpy of vaporization or heat capacity of the saturated liquid. Direct measurements of heat capacities provide useful checks on calculated heat capacities when they are available along a path traversing the temperature range of interest.

Tillner-Roth and Friend (1998a) have carried out a survey of the available literature for $NH_3 + H_2O$ mixtures. Their survey cites a total of three other publications (Chan and Giauque, 1964; Hildenbrand and Giauque, 1953; Wrewsky and Kaigorodoff, 1924) of heat capacity data and one publication of saturated-liquid enthalpy by Zinner (1934). The temperature range covered by published heat capacity data is 183 K to 334 K, with NH_3 compositions between 0.01 and 0.67 mole fraction. No heat capacities were found for NH_3-rich compostions at mole fractions above 0.67 or at temperatures above 334 K.

In this paper, heat capacities are reported for single-phase liquid and gaseous states from near ambient temperature to the upper limit of the apparatus (520 K). In addition, densities calculated from sample mass measurements and the volume of the calorimeter bomb are reported.

Experimental Section

Materials. High-purity samples of NH_3 and H_2O were obtained to prepare the mixtures. The NH_3 samples were drawn from a supply cylinder of anhydrous NH_3, with a certified minimum liquid purity of 0.9999 mole fraction. A gas chromatographic analysis confirmed this purity. Our H_2O supply was twice distilled in our laboratories and has a minimum purity of 0.9999 mole fraction.

The three mixtures of this study were prepared gravimetrically in clean, dry diaphragm cells constructed of Type-316 stainless steel. Each cell has a sample cavity above the diaphragm and a water-filled cavity below it, each having a volume of 100 cm^3. Water could be metered with a dual-piston pump into the lower cavity to raise and lower the diaphragm that separates the two chambers.

Prior to preparation of a mixture, calculations were made of the masses of NH_3 (M = 17.0303 g·mol^{-1}) and H_2O (M = 18.0153 g·mol^{-1}) required for the target composition. Then, each component was introduced to the upper chamber while the whole cell rested on an electronic platform balance capable of 0.1 g resolution. After each component was introduced, the whole cell was accurately weighed with a 25 kg capacity dual-pan balance whose resolution is 0.001 g and uncertainty is 0.005 g. After the final weighing, enough water was pumped into the lower chamber to pressurize the mixture above the diaphragm to 15 MPa. This pressure is well above the calculated bubble point pressure of the mixtures and thus promotes mixing of the two phases. Owing to the negative sign of the excess volume for $NH_3 + H_2O$ mixtures, the pressure fell as the sample was mixing. By monitoring the falling pressure of the water in the lower chamber, it was possible to determine that mixing was almost complete within 1 h. To ensure complete homogenization, each $NH_3 + H_2O$ mixture was then held for 2 weeks during which no further drift of pressure was detected. Following this holding period, each mixture was used in experiments. The masses and com-

* To whom correspondence should be addressed.
† Permanent address: Department of Applied Physics, The National Defense Academy, 1-10-20 Hashirimizu, Yokosuka 239, Japan.

10.1021/je980134g This article not subject to U.S. Copyright. Published 1998 by the American Chemical Society
Published on Web 10/15/1998

Table 1. Component Mass m, Mass Fraction NH_3 w, and Mole Fraction x of $\{xNH_3 + (1 - x)H_2O\}$ Mixtures Used in This Study

designation	$m(NH_3)$/g	$m(H_2O)$/g	x	w
80/20	56.623	13.372	0.817 50	0.808 96
90/10	57.676	6.434	0.904 60	0.899 64
70/30	58.913	24.936	0.714 22	0.702 61

positions of the mixtures used in this study are presented in Table 1.

Measurements. A twin-bomb adiabatic calorimeter was used for these measurements. Since this apparatus has been described in detail by Magee et al. (1998), only a brief discussion will be given here. A spherical bomb contains a sample of well-established mass. A second identical bomb serves as a reference. The volume of the bomb, approximately 70 cm^3, is a function of temperature and pressure. A platinum resistance thermometer is attached to the bomb for the temperature measurement. Temperatures are reported on the ITS-90, after conversions from the original calibration on the IPTS-68. Pressures are measured with an oscillating quartz crystal pressure transducer with a 0−70 MPa range. Adiabatic conditions are ensured by a high vacuum (3×10^{-3} Pa) in the vacuum space surrounding each calorimeter, by a temperature-controlled radiation shield, and by a temperature-controlled guard ring which thermally anchors the filling capillary and the lead wires to the bomb.

For the heat capacity measurement, a precisely determined electrical energy (Q) is applied and the resulting temperature rise ($\Delta T = T_2 - T_1$) is measured. We obtain the heat capacity from

$$c_V = \left(\frac{\partial U}{\partial T}\right)_V \cong \frac{\Delta Q - \Delta Q_0 - W_{pV}}{m\Delta T} \tag{2}$$

where U is the internal energy, $\Delta Q_0 = Q_{0,\mathrm{sam}} - Q_{0,\mathrm{ref}}$ is the energy difference between the sample and reference sides when both bombs are empty, $\Delta Q = Q_{\mathrm{sam}} - Q_{\mathrm{ref}}$ refers to the energy added during an experiment with a sample, W_{pV} is the change-of-volume work due to the slight dilation of the bomb, and m is the mass of substance enclosed in the sample bomb. In this work, the bomb was charged with sample up to the (p, T) conditions of the highest-density isochore to be measured. The bomb and its contents were cooled to a starting temperature in the single-phase liquid region. Then, measurements were performed in that region with increasing temperature until either the upper temperature (520 K) or pressure limit (20 MPa) was attained. At the completion of a run, a small part of the sample was cryopumped into a lightweight cylinder. The next run was started with a lower density. When the runs were completed, the remaining sample was discharged and weighed. A series of such runs from different fillings completes the investigation of the (p, T, c_V) surface. Each mass increment was determined from the difference of weighings of the lightweight cylinder made with a sensitive (10^{-3} g) balance. Small adjustments were made to each mass increment for changes in air buoyancy. The sample mass for each run was determined from the sum of the appropriate mass increments.

Assessment of Uncertainties. Uncertainty in the c_V determination has been discussed in detail (Magee et al., 1998). Primarily, the accuracy of this method is limited by the uncertainty involved in the temperature rise measurement and the change-of-volume work adjustment. We use a definition for the expanded uncertainty that is two times the standard uncertainty (i.e., a coverage factor k = 2 and thus a 2-standard-deviation estimate). The expanded uncertainties of the original measurements and the resulting combined uncertainties are shown in Table 2.

Table 2. Expanded Uncertainties of the Temperature, Pressure, Mass, Volume, Composition, Density, Energy, Change-of-Volume Work, and Specific Heat Capacity

temperature		density	0.2%
absolute	0.03 K	energy	
difference, ΔT	7×10^{-4} K	power	0.02%
pressure	0.007 MPa	difference, ΔQ	0.5 J·K^{-1}
mass	0.002 g	change-of-volume work	2%
volume	0.07 cm^3	specific heat capacity	
composition,	0.0002	liquid	1%
mass fraction		vapor	4%

Heat Capacity and Density Results

As mentioned in the discussion of eq 2, adjustments should be applied to the raw heat capacity data for the change-of-volume work of the bomb. During a measurement sequence, the volume of the bomb varies with temperature and pressure in accordance with formulas reported previously (Magee et al., 1998). The term W_{pV} is an important adjustment since the bomb is thin-walled. Referring to Goodwin and Weber (1969), we can obtain the work from

$$W_{pV} = \left(T_2\left(\frac{\partial p}{\partial T}\right)_{V_2} - \frac{1}{2}\Delta p\right)\Delta V \tag{3}$$

where $\Delta p = p_2 - p_1$ is the pressure rise and $\Delta V = V_2 - V_1$ is the change of volume. The pressure derivative is obtained from an equation of state. Accurate values for the pressure derivative were required, since this quantity has a significant influence on the adjustment for the change of volume work. Estimates of this derivative were calculated with an equation for the Helmholtz energy of NH_3 + H_2O mixtures developed by Tillner-Roth and Friend (1998b).

A minor adjustment is applied to the mass enclosed in the bomb. The total mass of the sample is corrected by deducting the mass residing in the noxious volume, which consists of the combined volumes of the connecting tubing, the charging valve body, and the pressure transducer. In total, the noxious volume is approximately 0.4% of the bomb volume. This amount is calculated from densities calculated with an equation of state (Tillner-Roth and Friend, 1998b) and the noxious volume obtained from previous calibrations (Magee et al., 1998).

The heat capacity data c_V of each run are presented in Table 3 for a total of 303 single-phase liquid and gaseous states. The final temperature (T, ITS-90) and pressure p of the heating interval are presented. The densities ρ of 359 states were calculated from the measured sample mass and the calibrated bomb volume at the measured temperatures and pressures. The measurements in Table 3 are presented in the order ($x \approx 0.8$, 0.9, and 0.7) in which the experiments were carried out. For each filling, up to five replicate runs were carried out in the same ranges of temperature and pressure. Table 3 presents the mean c_V of the replicate experiments at each temperature, calculated after dropping any c_V values that fell outside of the 95% confidence interval. The experimental densities and heat capacities are presented in the tables alongside values calculated with the formulation developed by Tillner-Roth and Friend (1998b).

Figures 1, 3, and 5 show the ranges of the measured temperatures and pressures along isochores and their relationship to calculated dew-bubble curves, for each composition. The measured pressures range up to 20 MPa,

Table 3. Experimental Densities ρ_{exp} and Heat Capacities c_V for $\{xNH_3 + (1 - x)H_2O\}$: x, mass fraction; T, Temperature on ITS-90; p, pressure; ρ_{calc} and $c_{V,calc}$ are Calculated with the Model of Tillner-Roth and Friend (1998b); dev. = 100 (exp − calc)/calc

T/K	p/MPa	ρ_{exp}/g·cm^3	ρ_{calc}/g·cm^3	dev.	c_V(no.1)[a]	c_V(no.2)	c_V(no.3)	c_V(no.4)	c_V(no.5)	$c_{V,avg}$	$c_{V,calc}$	dev.
					$x = 0.808\ 96$							
301	5.37	0.691 31	0.690 14	0.17								
302	7.10	0.691 12	0.690 13	0.14	3.348	3.337				3.343	3.362	−0.58
303	8.84	0.690 92	0.690 11	0.12	3.336	3.330				3.333	3.354	−0.63
304	10.57	0.690 73	0.690 08	0.09	3.323	3.339				3.331	3.346	−0.45
305	12.30	0.690 53	0.690 04	0.07	3.339	3.336				3.338	3.338	−0.01
306	14.03	0.690 34	0.690 00	0.05	3.340	3.333				3.336	3.331	0.17
307	15.76	0.690 14	0.689 95	0.03	3.348	3.362				3.355	3.323	0.96
308	17.48	0.689 95	0.689 90	0.01	3.357	3.353				3.355	3.316	1.18
309	19.20	0.689 75	0.689 83	−0.01	3.355	3.344				3.350	3.309	1.22
320	3.01	0.664 64	0.663 17	0.22								
321	4.59	0.664 47	0.663 21	0.19		3.175	3.202			3.189	3.354	−4.91
322	6.16	0.664 30	0.663 24	0.16		3.202	3.184			3.193	3.344	−4.53
323	7.72	0.664 12	0.663 25	0.13		3.205	3.200			3.202	3.335	−3.98
324	9.28	0.663 95	0.663 26	0.10		3.209	3.225			3.217	3.326	−3.28
325	10.85	0.663 78	0.663 26	0.08		3.235	3.242			3.239	3.318	−2.38
326	12.41	0.663 61	0.663 25	0.05	3.248	3.249	3.265			3.254	3.309	−1.67
327	13.96	0.663 44	0.663 24	0.03	3.277	3.272	3.280			3.276	3.301	−0.76
328	15.52	0.663 26	0.663 21	0.01	3.274	3.273	3.259			3.268	3.293	−0.76
329	17.07	0.663 09	0.663 18	−0.01	3.247	3.283	3.294			3.275	3.286	−0.33
330	18.62	0.662 92	0.663 15	−0.03	3.294	3.286	3.299			3.293	3.278	0.46
343	5.76	0.633 97	0.632 70	0.20								
344	7.14	0.633 82	0.632 77	0.17	3.286	3.233	3.223			3.247	3.3223	−2.26
345	8.51	0.633 67	0.632 81	0.14	3.256	3.268	3.247			3.257	3.3125	−1.68
346	9.89	0.633 53	0.632 85	0.11	3.236					3.236	3.3031	−2.03
347	11.26	0.633 38	0.632 88	0.08	3.274					3.274	3.2939	−0.6
348	12.63	0.633 23	0.632 90	0.05		3.257	3.250			3.253	3.2849	−0.97
349	14.00	0.633 08	0.632 91	0.03	3.269		3.249			3.259	3.2762	−0.53
350	15.37	0.632 93	0.632 92	0.00	3.248		3.257			3.253	3.2677	−0.46
351	16.74	0.632 79	0.632 92	−0.02	3.272	3.231	3.246			3.250	3.2595	−0.3
352	18.11	0.632 64	0.632 91	−0.04	3.242	3.225	3.228			3.231	3.2515	−0.62
353	19.48	0.632 49	0.632 89	−0.06	3.273	3.234	3.265			3.257	3.2436	0.42
361	6.78	0.606 78	0.605 36	0.24						3.257	3.2436	0.42
362	8.00	0.606 65	0.605 45	0.20	3.205	3.203				3.204	3.314	−3.30
363	9.22	0.606 52	0.605 53	0.16	3.198	3.177				3.188	3.303	−3.50
364	10.44	0.606 39	0.605 60	0.13	3.179	3.194				3.186	3.293	−3.25
365	11.65	0.606 26	.605 66	0.10	3.197	3.205				3.201	3.283	−2.51
366	12.87	0.606 13	0.605 70	0.07	3.206	3.203				3.204	3.274	−2.12
367	14.09	0.606 00	0.605 74	0.04	3.193	3.213				3.203	3.264	−1.89
368	15.30	0.605 88	0.605 77	0.02	3.191	3.203				3.197	3.255	−1.79
369	16.52	0.605 75	0.605 79	−0.01	3.220	3.239				3.230	3.247	−0.52
370	17.73	0.605 62	0.605 80	−0.03		3.245				3.245	3.238	0.23
371	18.97	0.605 49	0.605 84	−0.06	3.254					3.254	3.230	0.75
402	10.47	0.536 53	0.533 37	0.59								
403	11.34	0.536 44	0.533 51	0.55		3.179				3.179	3.329	−4.51
404	12.21	0.536 35	0.533 64	0.51		3.139				3.139	3.317	−5.36
405	13.07	0.536 26	0.533 75	0.47		3.182				3.182	3.305	−3.71
406	13.94	0.536 17	0.533 85	0.44	3.153	3.154	3.162			3.156	3.293	−4.16
407	14.81	0.536 09	0.533 94	0.40	3.154	3.149	3.166			3.156	3.282	−3.83
408	15.68	0.536 00	0.534 01	0.37	3.197	3.202	3.190			3.196	3.271	−2.29
409	16.55	0.535 91	0.534 08	0.34	3.168	3.195	3.183			3.182	3.261	−2.42
410	17.42	0.535 82	0.534 13	0.32	3.205	3.185	3.162			3.184	3.250	−2.05
411	18.30	0.535 73	0.534 19	0.29	3.185	3.181	3.152			3.173	3.240	−2.09
412	19.17	0.535 64	0.534 23	0.26	3.156	3.199	3.195			3.183	3.231	−1.46
442	15.33	0.443 55	0.438 78	1.09								
443	15.86	0.443 49	0.438 66	1.10	3.455					3.455	3.405	1.47
444	16.40	0.443 44	0.438 60	1.10	3.413	3.440	3.422			3.425	3.391	0.99
445	16.93	0.443 39	0.438 47	1.12	3.492	3.455	3.443			3.463	3.378	2.52
446	17.47	0.443 34	0.438 33	1.14	3.459	3.400	3.420			3.426	3.365	1.82
447	18.00	0.443 29	0.438 21	1.16	3.457	3.432	3.432			3.440	3.352	2.63
448	18.54	0.443 23	0.438 08	1.17	3.398	3.385	3.432			3.405	3.340	1.96
449	19.08	0.443 18	0.437 96	1.19	3.494	3.402	3.470			3.455	3.328	3.84
450	19.63	0.443 13	0.437 84	1.21	3.405		3.436			3.420	3.316	3.15
492	13.60	0.096 57	0.096 24	0.34								
493	13.68	0.096 56	0.096 29	0.28								
494	13.75	0.096 56	0.096 32	0.25								
495	13.83	0.096 55	0.096 34	0.22								
496	13.91	0.096 55	0.096 38	0.18								
497	13.99	0.096 54	0.096 42	0.13	3.288		3.603			3.445	2.797	23.17
498	14.07	0.096 54	0.096 42	0.13			3.402			3.402	2.790	21.94
499	14.15	0.096 53	0.096 46	0.07			3.396			3.396	2.783	22.04
500	14.22	0.096 53	0.096 49	0.04					3.382	3.382	2.776	21.81
501	14.30	0.096 52	0.096 52	0.00		3.422	3.456	3.396	3.347	3.405	2.769	22.96
502	14.38	0.096 52	0.096 55	−0.03				3.568	3.450	3.509	2.763	27.00

Table 3 (Continued)

T/K	p/MPa	ρ_{exp}/g·cm^3	ρ_{calc}/g·cm^3	dev.	c_V(no.1)[a]	c_V(no.2)	c_V(no.3)	c_V(no.4)	c_V(no.5)	$c_{V,avg}$	$c_{V,calc}$	dev.
503	14.46	0.096 51	0.096 57	−0.06		3.420	3.536		3.333	3.430	2.756	24.46
504	14.53	0.096 51	0.096 60	−0.10			3.368	3.383		3.376	2.750	22.75
505	14.61	0.096 50	0.096 63	−0.14	3.356		3.456	3.414		3.409	2.744	24.22
506	14.69	0.096 50	0.096 66	−0.16	3.306	3.445		3.388	3.321	3.365	2.738	22.89
507	14.77	0.096 49	0.096 68	−0.19	3.437	3.435	3.290		3.488	3.412	2.732	24.90
508	14.84	0.096 48	0.096 70	−0.22	3.353			3.431	3.417	3.400	2.726	24.73
509	14.92	0.096 48	0.096 73	−0.26	3.209	3.303	3.183			3.232	2.721	18.77
510	15.00	0.096 47	0.096 74	−0.28		3.291		3.282		3.286	2.715	21.03
511	15.07	0.096 47	0.096 77	−0.31		3.291	3.370	3.446	3.439	3.387	2.710	24.99
512	15.15	0.096 46	0.096 79	−0.35			3.312	3.370	3.292	3.324	2.704	22.93
513	15.23	0.096 46	0.096 82	−0.37		3.211		3.376	3.433	3.340	2.699	23.74
514	15.30	0.096 45	0.096 83	−0.39			3.161			3.161	2.694	17.35
515	15.38	0.096 45	0.096 86	−0.42		3.361		3.125	3.408	3.298	2.689	22.64
516	15.45	0.096 44	0.096 87	−0.45	3.267	3.243	3.095	3.125	3.092	3.164	2.684	17.89
517	15.53	0.096 44	0.096 89	−0.46		3.073	3.319	3.325		3.239	2.679	20.89
518	15.60	0.096 43	0.096 91	−0.49				3.321	2.949	3.135	2.675	17.20
519	15.68	0.096 43	0.096 93	−0.51		3.047				3.047	2.670	14.12
520	15.76	0.096 42	0.096 95	−0.55		3.339	3.025	3.291		3.218	2.666	20.72
521	15.83	0.096 42	0.096 96	−0.56	3.006				3.247	3.127	2.661	17.49
522	15.91	0.096 41	0.096 98	−0.59		3.125		3.107		3.116	2.657	17.26
$x = 0.899\ 64$												
301	3.63	0.648 43	0.646 39	0.32								
302	5.24	0.648 26	0.646 39	0.29								
303	6.84	0.648 09	0.646 38	0.26		3.077				3.077	3.167	−2.83
304	8.44	0.647 92	0.646 36	0.24	3.090	3.061				3.075	3.160	−2.67
305	10.04	0.647 75	0.646 34	0.22	3.086	3.104				3.095	3.153	−1.86
306	11.63	0.647 57	0.646 31	0.19	3.123	3.061				3.092	3.147	−1.76
307	13.23	0.647 4	0.646 29	0.17	3.094	3.086				3.090	3.141	−1.63
308	14.81	0.647 23	0.646 24	0.15	3.063	3.073				3.068	3.135	−2.14
309	16.40	0.647 06	0.646 20	0.13	3.085	3.069				3.077	3.129	−1.68
310	17.99	0.646 89	0.646 16	0.11	3.058	3.062				3.060	3.124	−2.05
311	19.58	0.646 72	0.646 11	0.09	3.092	3.090				3.091	3.118	−0.87
321	5.74	0.621 61	0.619 82	0.29								
322	7.17	0.621 46	0.619 84	0.26								
323	8.60	0.621 31	0.619 85	0.24	3.0687					3.069	3.134	−2.10
324	10.02	0.621 16	0.619 85	0.21	3.0677	3.0707				3.069	3.128	−1.86
325	11.44	0.621 01	0.619 85	0.19	3.0635	3.0729				3.068	3.121	−1.68
326	12.86	0.620 86	0.619 84	0.16	3.0745	3.0742				3.074	3.114	−1.28
327	14.28	0.620 71	0.619 83	0.14	3.0909					3.091	3.108	−0.54
328	15.70	0.620 56	0.619 80	0.12	3.0602	3.0656				3.063	3.102	−1.25
329	17.12	0.620 41	0.619 78	0.10	3.0883	3.0821				3.085	3.096	−0.34
330	18.53	0.620 27	0.619 75	0.08	3.0779	3.0850				3.081	3.090	−0.27
340	4.52	0.590 39	0.588 45	0.33								
341	5.76	0.590 26	0.588 51	0.30					3.029	3.029	3.135	−3.38
342	6.99	0.590 14	0.588 56	0.27		2.984				2.984	3.127	−4.58
343	8.22	0.590 01	0.588 59	0.24		3.007				3.007	3.119	−3.59
344	9.46	0.589 88	0.588 63	0.21	3.020	3.043				3.031	3.111	−2.58
345	10.69	0.589 76	0.588 65	0.19	3.014	3.003				3.008	3.104	−3.08
346	11.92	0.589 63	0.588 67	0.16	3.044	3.038				3.041	3.097	−1.80
347	13.15	0.589 50	0.588 68	0.14	3.024	3.017				3.021	3.090	−2.24
348	14.38	0.589 38	0.588 69	0.12	3.038	3.036				3.037	3.083	−1.50
349	15.61	0.589 25	0.588 69	0.10		3.045				3.045	3.076	−1.03
350	16.83	0.589 12	0.588 68	0.07	3.036	3.036				3.070	−1.10	
351	18.06	0.589 00	0.588 68	0.06	3.055	3.055				3.064	−0.29	
352	19.29	0.588 87	0.588 66	0.04	3.023	3.023				3.058	−1.13	
363	7.05	0.552 74	0.551 23	0.27								
364	8.08	0.552 64	0.551 30	0.24								
365	9.10	0.552 54	0.551 36	0.21	2.957	2.971				2.964	3.112	−4.76
366	10.13	0.552 43	0.551 41	0.18	2.971	2.980				2.976	3.104	−4.12
367	11.16	0.552 33	0.551 47	0.16	3.010	3.010				3.010	3.095	−2.74
368	12.19	0.552 23	0.551 50	0.13	2.967	3.009				2.988	3.087	−3.22
369	13.21	0.552 12	0.551 53	0.11	3.025	3.026				3.025	3.079	−1.75
370	14.24	0.552 02	0.551 56	0.08	2.966	2.977				2.971	3.072	−3.28
371	15.27	0.551 92	0.551 57	0.06	3.032					3.032	3.065	−1.08
372	16.29	0.551 82	0.551 59	0.04	2.993	3.008				3.000	3.058	−1.87
373	17.32	0.551 71	0.551 59	0.02	3.038	3.026				3.032	3.051	−0.61
374	18.35	0.551 61	0.551 60	0.00	2.990	3.000				2.995	3.044	−1.62
375	19.37	0.551 51	0.551 59	−0.01	3.007	3.016				3.012	3.037	−0.85
401	11.35	0.474 99	0.474 88	0.02								
402	12.04	0.474 92	0.474 90	0.00								
403	12.72	0.474 85	0.474 91	−0.01								
404	13.41	0.474 79	0.474 91	−0.03								
405	14.09	0.474 72	0.474 91	−0.04		3.226				3.226	3.118	3.48
406	14.78	0.474 66	0.474 90	−0.05	3.180	3.202				3.191	3.108	2.66
407	15.46	0.474 59	0.474 88	−0.06		3.173	3.211			3.192	3.099	3.01
408	16.15	0.474 52	0.474 87	−0.07		3.165	3.177			3.171	3.090	2.63

Table 3 (Continued)

T/K	p/MPa	ρ_{exp}/g·cm^3	ρ_{calc}/g·cm^3	dev.	c_V(no.1)[a]	c_V(no.2)	c_V(no.3)	c_V(no.4)	c_V(no.5)	$c_{V,avg}$	$c_{V,calc}$	dev.
409	16.84	0.474 46	0.474 83	−0.08		3.152	3.158			3.155	3.081	2.40
410	17.53	0.474 39	0.474 81	−0.09	3.163	3.166	3.148			3.159	3.073	2.81
411	18.23	0.474 32	0.474 77	−0.10		3.166				3.166	3.064	3.32
412	18.92	0.474 26	0.474 74	−0.10	3.150	3.185	3.156			3.163	3.056	3.51
413	19.62	0.474 19	0.474 70	−0.11	3.135	3.133				3.134	3.048	2.81
421	13.67	0.416 88	0.418 69	−0.43								
422	14.16	0.416 84	0.418 48	−0.39								
423	14.65	0.416 79	0.418 25	−0.35		3.354				3.354	3.205	4.65
424	15.15	0.416 74	0.418 04	−0.31	3.375	3.375				3.375	3.194	5.68
425	15.65	0.416 70	0.417 84	−0.27	3.310	3.400				3.355	3.182	5.43
426	16.15	0.416 65	0.417 66	−0.24	3.364					3.364	3.171	6.09
427	16.65	0.416 60	0.417 46	−0.20	3.335	3.351				3.343	3.160	5.77
428	17.16	0.416 56	0.417 28	−0.17		3.304				3.304	3.150	4.89
429	17.66	0.416 51	0.417 10	−0.14	3.276	3.358				3.317	3.139	5.67
430	18.17	0.416 46	0.416 93	−0.11	3.278	3.311				3.294	3.129	5.28
431	18.68	0.416 42	0.416 76	−0.08	3.320	3.289				3.305	3.119	5.94
432	19.19	0.416 37	0.416 59	−0.05	3.316	3.269				3.293	3.110	5.88
433	19.70	0.416 32	0.416 42	−0.02	3.256	3.247				3.252	3.100	4.88
441	15.53	0.311 41	0.320 06	−2.70								
442	15.81	0.311 38	0.318 69	−2.29	4.203					4.203	3.426	22.68
443	16.09	0.311 36	0.317 41	−1.91	4.286					4.286	3.412	25.65
444	16.37	0.311 34	0.316 25	−1.55	4.129					4.129	3.397	21.54
445	16.66	0.311 32	0.315 23	−1.24	4.111					4.111	3.382	21.55
446	16.94	0.311 3	0.314 28	−0.95	4.027					4.027	3.368	19.58
447	17.23	0.311 28	0.313 40	−0.68	3.991					3.991	3.353	19.02
448	17.52	0.311 25	0.312 57	−0.42	3.926					3.926	3.338	17.59
449	17.81	0.311 23	0.311 85	−0.20	3.990					3.990	3.324	20.03
450	18.10	0.311 21	0.311 15	0.02	3.879					3.879	3.310	17.20
451	18.39	0.311 18	0.310 49	0.22	3.818					3.818	3.295	15.86
452	18.69	0.311 16	0.309 91	0.40	3.727					3.727	3.281	13.59
453	18.98	0.311 14	0.309 36	0.58	3.744					3.744	3.268	14.59
454	19.28	0.311 11	0.308 85	0.73	3.616					3.616	3.254	11.12
455	19.57	0.311 09	0.308 35	0.89	3.639					3.639	3.241	12.29
456	19.87	0.311 07	0.307 91	1.03	3.566					3.566	3.228	10.49
448	15.65	0.241 27	0.258 58	−6.69								
449	15.85	0.241 26	0.256 91	−6.09								
450	16.06	0.241 25	0.255 46	−5.56								
451	16.26	0.241 24	0.254 13	−5.07								
452	16.47	0.241 23	0.252 95	−4.63	4.307	4.494	4.488			4.430	3.448	28.46
453	16.68	0.241 22	0.251 87	−4.23	4.266	4.476	4.397			4.380	3.429	27.72
454	16.89	0.241 21	0.250 88	−3.85	4.245	4.437	4.364			4.349	3.411	27.50
455	17.10	0.241 19	0.249 91	−3.49	4.173	4.230	4.253			4.219	3.392	24.37
456	17.31	0.241 18	0.249 03	−3.15	4.148	3.997	4.082			4.076	3.374	20.80
457	17.52	0.241 17	0.248 23	−2.84	3.935	4.184	4.051			4.057	3.356	20.88
458	17.73	0.241 16	0.247 47	−2.55	3.924	3.967	4.047			3.979	3.338	19.19
459	17.94	0.241 14	0.246 80	−2.29	3.978	3.905	3.942			3.942	3.321	18.68
460	18.15	0.241 13	0.246 16	−2.04		3.850				3.850	3.305	16.49
461	18.36	0.241 11	0.245 57	−1.82	3.866	3.809	4.065			3.913	3.288	18.99
462	18.58	0.241 10	0.244 99	−1.59	3.784	3.820	3.857			3.820	3.273	16.73
463	18.79	0.241 08	0.244 48	−1.39	3.725	3.777	3.942			3.815	3.258	17.11
464	19.00	0.241 07	0.243 98	−1.19	3.652	3.689	3.723			3.688	3.243	13.73
465	19.22	0.241 06	0.243 52	−1.01	3.701	3.772	3.752			3.741	3.228	15.90
466	19.43	0.241 04	0.243 09	−0.84	3.663	3.609	3.667			3.646	3.214	13.44
467	19.64	0.241 02	0.242 69	−0.69	3.541	3.669	3.628			3.613	3.201	12.88
468	19.86	0.241 01	0.242 29	−0.53	3.470	3.545	3.615			3.544	3.188	11.17
452	15.30	0.191 87	0.209 13	−8.25								
453	15.46	0.191 86	0.207 91	−7.72								
454	15.63	0.191 85	0.206 86	−7.26								
455	15.79	0.191 85	0.205 83	−6.79	4.588	4.362	4.619			4.523	3.415	32.45
456	15.95	0.191 84	0.204 89	−6.37	4.575	4.499	4.477			4.517	3.393	33.11
457	16.12	0.191 83	0.204 06	−5.99	4.48	4.225	4.271			4.325	3.373	28.26
458	16.29	0.191 83	0.203 27	−5.63	4.472	4.191	4.108			4.257	3.352	26.98
459	16.45	0.191 82	0.202 55	−5.30	4.495	4.154	4.136			4.262	3.333	27.87
460	16.62	0.191 81	0.201 88	−4.99	4.234	4.113	4.015			4.121	3.314	24.32
461	16.78	0.191 80	0.201 26	−4.70	4.268	4.127	4.123			4.173	3.296	26.58
462	16.95	0.191 79	0.200 67	−4.43	4.120	3.984	4.087			4.064	3.279	23.93
463	17.11	0.191 78	0.200 15	−4.18	4.141	4.025	4.071			4.079	3.262	25.03
464	17.28	0.191 78	0.199 61	−3.92	3.991	3.815	4.037			3.948	3.246	21.64
465	17.44	0.191 77	0.199 13	−3.70	3.924	3.810	3.847			3.861	3.230	19.53
466	17.61	0.191 76	0.198 67	−3.48	3.834		3.659			3.746	3.214	16.55
467	17.77	0.191 75	0.198 26	−3.28	3.883	3.743	3.782			3.803	3.199	18.86
468	17.94	0.191 74	0.197 86	−3.09	3.885	3.637	3.761			3.185	18.09	
469	18.10	0.191 73	0.197 48	−2.91	3.979	3.653	3.717			3.783	3.171	19.30
470	18.27	0.191 72	0.197 13	−2.75	3.697	3.584	3.669			3.650	3.157	15.61
471	18.44	0.191 71	0.196 83	−2.60	3.648	3.693				3.670	3.144	16.75
472	18.60	0.191 69	0.196 51	−2.45	3.719	3.558	3.540			3.606	3.131	15.18

Table 3 (Continued)

T/K	p/MPa	ρ_{exp}/g·cm^3	ρ_{calc}/g·cm^3	dev.	c_V(no.1)[a]	c_V(no.2)	c_V(no.3)	c_V(no.4)	c_V(no.5)	$c_{V,avg}$	$c_{V,calc}$	dev.
473	18.77	0.191 68	0.196 21	−2.31	3.768	3.451	3.608			3.609	3.118	15.75
474	18.93	0.191 67	0.195 94	−2.18	3.651	3.428	3.507			3.529	3.105	13.63
475	19.10	0.191 66	0.195 67	−2.05	3.655	3.406	3.480			3.513	3.093	13.58
476	19.26	0.191 65	0.195 43	−1.94	3.730	3.390	3.768			3.629	3.082	17.77
477	19.43	0.191 64	0.195 20	−1.83	3.684	3.386	3.585			3.552	3.070	15.68
478	19.60	0.191 63	0.194 98	−1.72	3.558	3.327	3.570			3.485	3.059	13.93
479	19.76	0.191 62	0.194 76	−1.61	3.623	3.437	3.472			3.511	3.048	15.17
480	19.93	0.191 61	0.194 55	−1.51	3.652	3.358	3.518			3.509	3.038	15.53
461	14.38	0.129 58	0.130 38	−0.62	3.743	3.524	3.683			3.650	3.065	19.09
462	14.49	0.129 57	0.130 33	−0.58	3.766	3.541	3.891			3.732	3.052	22.31
463	14.60	0.129 56	0.130 29	−0.56	3.717	3.566	3.797			3.693	3.039	21.54
464	14.71	0.129 56	0.130 26	−0.54	3.460	3.501	3.442			3.468	3.026	14.60
465	14.82	0.129 55	0.130 22	−0.51	3.758	3.498	3.289			3.515	3.014	16.64
466	14.93	0.129 54	0.130 20	−0.51	3.487	3.624	3.651			3.587	3.002	19.49
467	15.03	0.129 54	0.130 16	−0.48	3.609	3.425	3.621			3.551	2.990	18.78
468	15.14	0.129 53	0.130 15	−0.48	3.611		3.376			3.494	2.979	17.27
469	15.25	0.129 52	0.130 09	−0.44		3.213	3.824			3.518	2.968	18.55
470	15.36	0.129 52	0.130 09	−0.44	3.248	3.271	3.722			3.414	2.957	15.43
471	15.47	0.129 51	0.130 09	−0.45	3.733	3.335	3.621			3.563	2.947	20.90
472	15.58	0.129 50	0.130 05	−0.43	3.635	3.425	3.392			3.484	2.937	18.63
473	15.68	0.129 49	0.130 04	−0.42	3.365	3.538	3.395			3.433	2.927	17.29
474	15.79	0.129 49	0.130 01	−0.40	3.379	3.495	3.288			3.387	2.917	16.12
475	15.90	0.129 48	0.129 97	−0.38	3.345	3.267	3.109			3.240	2.908	11.44
476	16.00	0.129 47	0.129 96	−0.38	3.219	3.317	3.405			3.314	2.898	14.33
477	16.11	0.129 47	0.129 94	−0.36	3.640	3.195	3.624			3.486	2.889	20.66
478	16.22	0.129 46	0.129 92	−0.35	3.504	3.351	3.195			3.350	2.880	16.31
479	16.32	0.129 45	0.129 90	−0.34	3.785	3.188	3.425			3.466	2.872	20.70
480	16.43	0.129 44	0.129 87	−0.33	3.358	3.367	3.379			3.368	2.863	17.63
481	16.54	0.129 44	0.129 86	−0.32	3.441	3.159	3.575			3.391	2.855	18.77
482	16.64	0.129 43	0.129 85	−0.33	3.320	3.361	3.374			3.352	2.848	17.71
483	16.75	0.129 42	0.129 84	−0.32	3.668	3.203	3.458			3.443	2.840	21.23
484	16.85	0.129 41	0.129 84	−0.33	3.378	3.126	3.368			3.291	2.833	16.17
485	16.96	0.129 41	0.129 83	−0.32	3.426	3.231	3.258			3.305	2.825	17.00
486	17.07	0.129 40	0.129 81	−0.32	3.286	3.130	3.192			3.203	2.818	13.66
487	17.17	0.129 39	0.129 80	−0.32	3.298	3.066	3.320			3.228	2.811	14.85
488	17.28	0.129 39	0.129 78	−0.30	3.256	3.117	3.290			3.221	2.804	14.89
489	17.38	0.129 38	0.129 78	−0.31	3.458	3.425	3.140			3.341	2.797	19.44
490	17.49	0.129 37	0.129 78	−0.32	3.141	3.228	3.060			3.143	2.791	12.62
491	17.59	0.129 36	0.129 79	−0.33	3.431	2.961	3.448			3.280	2.784	17.79
492	17.70	0.129 36	0.129 75	−0.30	3.156	3.524	3.177			3.285	2.778	18.26
493	17.80	0.129 35	0.129 72	−0.29	3.558	2.986	3.206			3.250	2.772	17.26
494	17.91	0.129 34	0.129 72	−0.30	3.063	2.992	3.062			3.039	2.766	9.87
495	18.01	0.129 33	0.129 74	−0.32		3.190	3.147			3.168	2.761	14.78
496	18.12	0.129 33	0.129 73	−0.31	3.086	3.401	3.403			3.297	2.755	19.67
497	18.22	0.129 32	0.129 73	−0.32	3.176	3.312	3.256			3.248	2.749	18.14
498	18.32	0.129 31	0.129 71	−0.31	3.049		3.256			3.152	2.744	14.89
499	18.43	0.129 30	0.129 70	−0.31	2.903	2.736	3.486			3.042	2.739	11.06
500	18.53	0.129 30	0.129 69	−0.30	2.694	3.504	3.387			3.195	2.734	16.86
501	18.64	0.129 29	0.129 67	−0.30	2.912		3.392			3.152	2.729	15.50
503	18.84	0.129 27	0.129 67	−0.31	3.052	3.181	3.331			3.188	2.719	17.24
504	18.95	0.129 27	0.129 66	−0.30	3.279	2.929				3.104	2.715	14.33
505	19.05	0.129 26	0.129 66	−0.31	3.087	2.946	3.409			3.147	2.710	16.15
506	19.15	0.129 25	0.129 65	−0.31	3.325	2.997				3.161	2.706	16.81
507	19.26	0.129 24	0.129 66	−0.33	3.198	3.262	3.258			3.239	2.701	19.91
510	19.57	0.129 22	0.129 65	−0.33	2.945	3.394	3.278			3.205	2.689	19.20
511	19.67	0.129 21	0.129 63	−0.33	2.932	3.035	3.170			3.045	2.685	13.41
512	19.77	0.129 21	0.129 62	−0.31			3.154			3.154	2.681	17.64
						$x = 0.702\ 61$						
307	8.97	0.7353	0.7345	0.10								
308	10.80	0.7351	0.7344	0.09								
309	12.62	0.7348	0.7343	0.07		3.523				3.523	3.443	2.31
310	14.44	0.7346	0.7342	0.06	3.518	3.518	3.517			3.518	3.437	2.36
311	16.26	0.7344	0.7341	0.04	3.539	3.542	3.530	3.521		3.533	3.430	3.00
312	18.07	0.7342	0.7340	0.03	3.524	3.508	3.502	3.497		3.508	3.424	2.46
322	4.62	0.71462	0.71398	0.09								
323	6.33	0.71442	0.71391	0.07								
324	8.04	0.71422	0.71383	0.05	3.444	3.4571	3.4692			3.457	3.436	0.61
325	9.74	0.71402	0.71374	0.04	3.500	3.4941	3.4875			3.494	3.428	1.92
326	11.44	0.71382	0.71365	0.02	3.500	3.5065				3.503	3.421	2.42
327	13.13	0.71363	0.71356	0.01	3.539	3.5301	3.5103			3.527	3.413	3.32
328	14.83	0.71343	0.71346	0.00	3.506	3.5200	3.5071			3.511	3.406	3.08
329	16.52	0.71323	0.71335	−0.02	3.508	3.5102	3.5135			3.511	3.399	3.28
330	18.21	0.71303	0.71324	−0.03	3.538	3.5336	3.5263			3.533	3.392	4.14
344	4.78	0.68599	0.68575	0.03								
345	6.32	0.68582	0.68570	0.02								
346	7.85	0.68564	0.68565	0.00								

Table 3 (Continued)

T/K	p/MPa	ρ_{exp}/g·cm^3	ρ_{calc}/g·cm^3	dev.	c_V(no.1)[a]	c_V(no.2)	c_V(no.3)	c_V(no.4)	c_V(no.5)	$c_{V,avg}$	$c_{V,calc}$	dev.
347	9.38	0.68547	0.68558	−0.02	3.478	3.485	3.476			3.480	3.400	2.35
348	10.91	0.68529	0.68552	−0.03	3.486	3.505	3.500			3.497	3.392	3.09
349	12.44	0.68512	0.68545	−0.05	3.486	3.500	3.509			3.498	3.384	3.37
350	13.97	0.68495	0.68537	−0.06	3.510	3.498	3.488			3.498	3.376	3.61
351	15.49	0.68477	0.68528	−0.07	3.495	3.504	3.502			3.500	3.369	3.90
352	17.01	0.68460	0.68520	−0.09	3.480	3.491	3.476			3.482	3.362	3.59
353	18.54	0.684 42	0.685 11	−0.10	3.499	3.489	3.500			3.496	3.354	4.23
363	5.91	0.660 00	0.659 96	0.01								
364	7.29	0.659 84	0.659 94	−0.02								
365	8.68	0.659 69	0.659 91	−0.03								
366	10.06	0.659 53	0.659 87	−0.05	3.447	3.449	3.432			3.443	3.379	1.88
367	11.44	0.659 38	0.659 82	−0.07	3.439	3.437	3.451			3.442	3.371	2.13
368	12.82	0.659 22	0.659 77	−0.08	3.451	3.441	3.430			3.441	3.362	2.34
369	14.20	0.659 07	0.659 71	−0.10	3.494	3.483	3.478			3.485	3.354	3.91
370	15.58	0.658 91	0.659 64	−0.11	3.411	3.415	3.421			3.416	3.346	2.08
371	16.95	0.658 76	0.659 57	−0.12	3.484	3.482	3.493			3.486	3.339	4.43
372	18.33	0.658 61	0.659 50	−0.13	3.424	3.424	3.430			3.426	3.331	2.85
373	19.71	0.658 45	0.659 42	−0.15	3.469	3.474	3.469			3.471	3.324	4.43
382	7.43	0.632 25	0.632 09	0.03								
383	8.67	0.632 12	0.632 10	0.00								
384	9.90	0.631 98	0.632 09	−0.02	3.388	3.401	3.411			3.400	3.376	0.71
385	11.13	0.631 85	0.632 07	−0.04	3.442	3.428	3.398			3.423	3.367	1.66
386	12.36	0.631 71	0.632 05	−0.05	3.428	3.436	3.442			3.435	3.358	2.31
387	13.59	0.631 58	0.632 02	−0.07	3.433	3.415	3.435			3.428	3.349	2.35
388	14.82	0.631 44	0.631 98	−0.09	3.399	3.397	3.406			3.401	3.340	1.82
389	16.05	0.631 31	0.631 94	−0.10	3.419	3.419	3.452			3.430	3.332	2.95
390	17.28	0.631 17	0.631 89	−0.11	3.400	3.416				3.408	3.323	2.55
391	18.51	0.631 04	0.631 84	−0.13	3.397	3.404	3.386			3.396	3.315	2.42
392	19.74	0.630 90	0.631 78	−0.14	3.389	3.468				3.429	3.307	3.67
412	9.19	0.580 66	0.579 63	0.18								
413	10.04	0.580 57	0.579 43	0.20								
414	10.98	0.580 47	0.579 41	0.18								
415	11.94	0.580 36	0.579 4	0.17								
416	12.91	0.580 26	0.579 43	0.14								
417	13.89	0.580 16	0.579 45	0.12	3.424	3.324				3.374	3.369	0.14
418	14.86	0.580 05	0.579 47	0.10	3.392	3.364				3.378	3.359	0.57
419	15.84	0.579 95	0.579 48	0.08		3.339				3.339	3.349	−0.29
420	16.83	0.579 84	0.579 48	0.06		3.327				3.327	3.339	−0.38
421	17.81	0.579 74	0.579 47	0.05	3.375	3.329				3.352	3.330	0.67
422	18.79	0.579 64	0.579 45	0.03	3.320	3.361				3.340	3.320	0.61
423	19.77	0.579 53	0.579 44	0.02	3.354	3.344				3.349	3.311	1.13
443	14.81	0.525 45	0.522 9	0.49								
444	15.57	0.525 37	0.522 95	0.46								
445	16.31	0.525 29	0.522 95	0.45		3.421				3.421	3.410	0.31
446	17.07	0.525 21	0.522 95	0.43			3.358	3.387		3.373	3.399	−0.77
447	17.82	0.525 14	0.522 94	0.42	3.360	3.328				3.344	3.387	−1.28
448	18.57	0.525 06	0.522 93	0.41	3.299	3.253	3.268			3.273	3.376	−3.06
449	19.33	0.524 98	0.522 91	0.40		3.312	3.318			3.315	3.365	−1.50
465	15.65	0.464 55	0.458 01	1.43								
466	16.18	0.464 50	0.457 73	1.48	3.506	3.497				3.502	3.538	−1.03
467	16.72	0.464 44	0.457 48	1.52		3.479				3.479	3.525	−1.30
468	17.26	0.464 39	0.457 26	1.56		3.452				3.452	3.512	−1.69
469	17.80	0.464 34	0.457 05	1.60	3.400	3.378				3.389	3.498	−3.13
470	18.35	0.464 28	0.456 86	1.62	3.328	3.294				3.311	3.486	−5.01
471	18.90	0.464 22	0.456 69	1.65	3.305	3.319				3.312	3.473	−4.62
472	19.45	0.464 17	0.456 52	1.68		3.236				3.236	3.460	−6.47

[a] All c_V values in kJ·kg^{-1}·K^{-1}.

which leaves only a narrow gap above the bubble-point pressures at temperatures above about 425 K. Figures 2, 4, and 6 show the measured specific heat capacities for each of the compositons. At densities $\rho > \sim 1.3\rho_c$, the liquid-phase c_V values show only weak dependence on both density and temperature with the appearance of a shallow minimum heat capacity. The minima range from about (3.0 to 3.3) kJ·kg^{-1}·K^{-1} as the mole fraction (x) of ammonia decreases from 0.9 to 0.7 in the mixture. Compressed-gas heat capacities for the $x \approx 0.8$ and $x \approx 0.9$ mixtures show a significantly stronger rate of change with temperature. In this case, the c_V values range from (2.7 to 4.5) kJ·kg^{-1}·K^{-1}.

As shown in Table 2, the uncertainty of values of c_V for gases is about four times that for liquid-phase results. This is due to the higher relative uncertainty of the ΔQ term for gaseous measurements. Consequently, the gas-phase c_V data have considerably more scatter than the liquid-phase data. Figures 2 and 4 indicate that this scatter is a factor of about 10 larger in the gas than in the liquid. We think that this scatter is due to the combination of two effects. The first is the considerably higher electrical noise originating with thermal EMFs at temperatures above 425 K. The second is the much lower measured energy changes, which were a factor of 10 smaller than for liquid-phase samples. While we can certainly conceive techniques to reduce noise, the second effect cannot be mitigated for an apparatus of fixed volume. Electrical noise destabilizes the control algorithm and causes spurious losses or gains of energy that cannot be calculated. This noise arises when

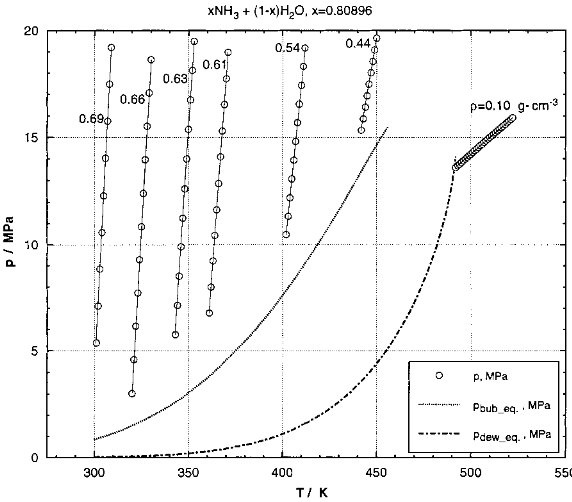

Figure 1. Measured pressure and temperature states along isochores for $\{x NH_3 + (1 - x)H_2O, x = 0.808\ 96\}$, showing the dew-bubble curves calculated with a formulation by Tillner-Roth and Friend (1998b).

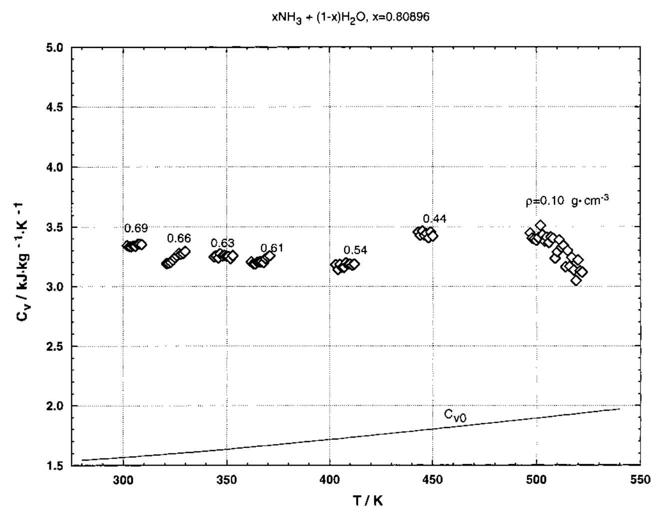

Figure 2. Measured specific heat at constant volume c_V for $\{x NH_3 + (1 - x)H_2O, x = 0.808\ 96\}$, showing the ideal gas heat capacity c_V° calculated with a formulation by Tillner-Roth and Friend (1998b).

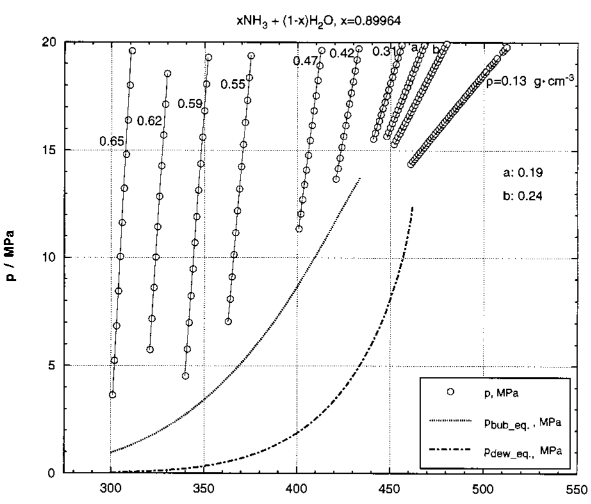

Figure 3. Measured pressure and temperature states along isochores for $\{x NH_3 + (1 - x)H_2O, x = 0.899\ 64\}$, showing the dew-bubble curves calculated with a formulation by Tillner-Roth and Friend (1998b).

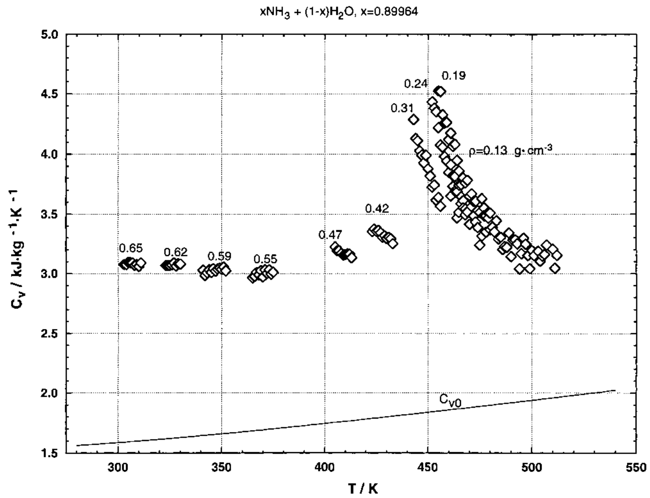

Figure 4. Measured specific heat at constant volume c_V for $\{x NH_3 + (1 - x)H_2O, x = 0.899\ 64\}$, showing the ideal gas heat capacity c_V° calculated with a formulation by Tillner-Roth and Friend (1998b).

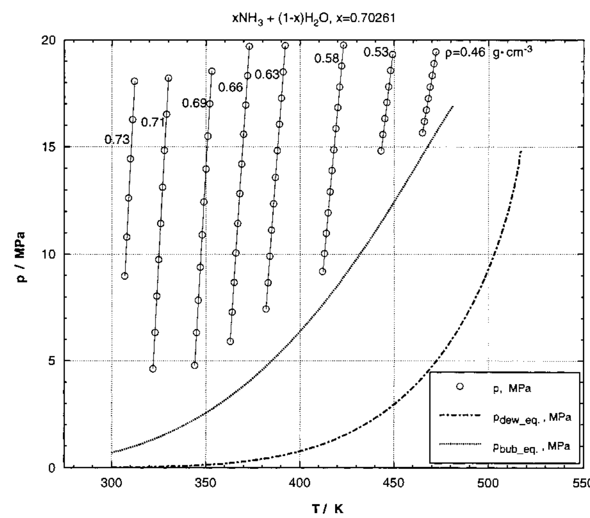

Figure 5. Measured pressure and temperature states along isochores for $\{x NH_3 + (1 - x)H_2O, x = 0.702\ 61\}$, showing the dew-bubble curves calculated with a formulation by Tillner-Roth and Friend (1998b).

crimped electrical connections loosen at elevated temperatures. Loose connectors generate electrical noise, which can swamp the nanovolt signals that we are attempting to measure. For future studies, modifications are being made to reduce thermal emf's in the measuring circuits by replacing crimped connectors with cleaned and carefully soldered connections. Preliminary tests lead us to be optimistic that this will decrease the scatter of gas-phase c_V to a more satisfactory value.

Table 3 presents comparisons of calculated densities and heat capacities with experimental values from this work. The calculations were made with a formulation developed by Tillner-Roth and Friend (1998b). This formulation was developed by using published thermodynamic measurements that were available at temperatures up to 334 K for heat capacity and up to 413 K for density. Above such temperatures, the calculations are an extrapolation of the available data along the lines of the formulation. Table 3 shows that the calculated densities are within ±0.3% at temperatures up to 400 K, within ±8% in the extended critical region, and within ±0.6% in the supercritical gas region. Also, Table 3 shows that the calculated heat

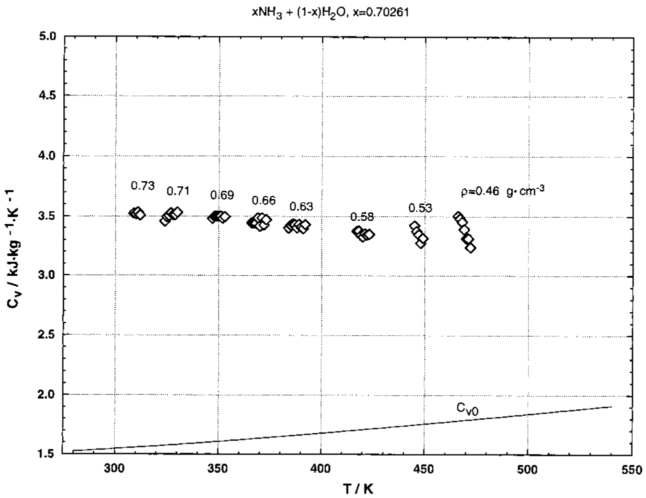

Figure 6. Measured specific heat at constant volume c_V for $\{xNH_3 + (1 - x)H_2O, x = 0.702\ 61\}$, showing the ideal gas heat capacity c_V° calculated with a formulation by Tillner-Roth and Friend (1998b).

capacities are within ±5% at all state conditions except the extended critical and supercritical gas regions, where they are within ±30%. Since the present data were not available to Tillner-Roth and Friend, it is perhaps not surprising that the deviations often exceed the uncertainty of the measurements. On the other hand, considering how most of the calculated densities and heat capacites are an extrapolation of the published data, the agreement of the calculations with experiment is good.

Acknowledgment

We are grateful to Dan Friend, Adam Nowarski, Reiner Tillner-Roth, Torsten Lüddecke, and Mark McLinden for generous technical assistance and helpful discussions during this study.

Literature Cited

Chan, J. P.; Giauque, W. F. The entropy of $NH_3{\cdot}2H_2O$. Heat Capacity from 15 to 300 K. *J. Phys. Chem.* **1964**, *68*, 3053−3057.

Goodwin, R. D.; Weber, L. A. Specific Heats C_v of Fluid Oxygen from the Triple Point to 300 K at Pressures to 350 Atmospheres. *J. Res. Natl. Bur. Stand.* **1969**, *73A*, 15−24.

Hildenbrand, D. L.; Giauque, W. F. Ammonium oxide and ammonium hydroxide. Heat capacities and thermodynamic properties from 15 to 300 K. *J. Am. Chem. Soc.* **1953**, *75*, 2811−2818.

Magee, J. W.; Blanco, J. C.; Deal, R. J. High-Temperature Adiabatic Calorimeter for Constant-Volume Heat Capacity of Compressed Gases and Liquids. *J. Res. Natl. Inst. Stand. Technol.* **1998**, *103*, 63−75.

Tillner-Roth, R.; Friend, D. G. Survey and Assessment of Available Measurements on Thermodynamic Properties of the Mixture {Water + Ammonia}. *J. Phys. Chem. Ref. Data* **1998a**, *27*, 45−61.

Tillner-Roth, R.; Friend, D. G. A Helmholtz Free Energy Formulation of the Thermodynamic Properties of the Mixture {Water + Ammonia}. *J. Phys. Chem. Ref. Data* **1998b**, *27*, 63−77.

Wrewsky, M.; Kaigorodoff, A. I. Heat Capacity of Aqueous Solutions with Hydrogen Chloride and Ammonia at Several Temperatures. *Z. Phys. Chem.* **1924**, *112*, 83−89.

Zinner, K. Enthalpy of Mixtures of Ammonia and Water: Dependence on Composition and Temperature. *Z. Gesamte Kalte-Ind.* **1934**, *41*, 21−29.

Received for review June 16, 1998. Accepted September 7, 1998. This research project was supported by grants from the U. S. Department of Energy, Geothermal Division and from ABB Power Plant Laboratories/ Combustion Engineering, Inc.

JE980134G